Inflammation Research (2026) 75:70
https://doi.org/10.1007/s00011-026-02209-6

Inflammation Research

RESEARCH

Multi-dimensional plasma proteomic profiling elucidates molecular mechanisms and pathophysiological networks in pediatric severe traumatic brain injury

Enis Cela[1] · David Tweddell[2] · Mark Daley[2,3] · Maria Morello[4] · Gediminas Cepinskas[5,6,7] · Douglas D. Fraser[1,7,8,9,10,11,12]

Received: 31 October 2025 / Revised: 13 February 2026 / Accepted: 14 February 2026

Abstract

Background Severe traumatic brain injury (sTBI) is a leading cause of trauma-related mortality and morbidity in pediatric populations. The heterogeneous progression of sTBI presents significant challenges for prognosis and pathophysiological investigation, necessitating advances beyond traditional approaches. This study utilized plasma proteomic profiling to identify sTBI-specific protein alterations and functional pathways correlating with clinical variables in pediatric patients.

Methods We performed plasma proteomic analysis on 20 matched pairs of pediatric sTBI patients and healthy controls. Proximity extension assays quantified 1,472 proteins. Gene set enrichment analysis identified enriched Reactome pathways and Gene Ontology terms among differentially expressed proteins. Pathway-clinical variable associations were calculated using weighted correlation sums between pathway proteins and clinical variables. Protein-protein interaction networks were analyzed using STRING.

Results Using significance thresholds of FDR-adjusted $P < 0.05$ and fold change ≥ 4, we identified 65 differentially expressed proteins between sTBI samples and controls. Analysis revealed proteins involved in neuroinflammation and upregulated pathways related to cytokine and receptor/ligand signaling. Altered protein expression indicated structural and functional changes in neurons, glial cells, and vasculature. Upregulated pathways positively correlated with injury severity score, hyperglycemia, and coagulopathy, while negatively correlating with vault skull fractures and acidosis. IL-6 emerged as a central hub in protein-protein interactions, with distinct clusters representing opsonization, TNF family signaling, amidation, neuronal/astrocyte injury, and multifaceted sTBI responses.

Conclusions These findings identify differentially expressed plasma proteins and enriched signaling pathways associated with clinical features, providing novel insights into pediatric sTBI pathophysiology. The identification of IL-6 as a central hub protein and the correlation of specific pathways with injury severity, metabolic dysfunction, and coagulopathy suggest potential targets for therapeutic intervention and prognostic biomarker development. This proteomic approach advances our understanding of the complex molecular cascades underlying pediatric sTBI and may inform precision medicine strategies for improved patient outcomes.

Keywords Pediatric · Traumatic brain injury · Proteomics · Pathways · Protein alterations · Inflammation

Abbreviations

ADAM22	Disintegrin and metalloproteinase domain-containing protein 22
ADM	Adrenomedullin
CALB1	Calbindin 1
CALCA	Calcitonin-related polypeptide alpha
CCL	Chemokine (C-C motif) ligand
CRH	Corticotropin-releasing hormone
CRP	C-reactive protein
CSF3	Colony-stimulating factor 3
CT	Computed tomography
DEPs	Differentially expressed proteins

Communicated by Jianxiong Jiang

Extended author information available on the last page of the article

Published online: 27 March 2026

FDR	False discovery rate
GCS	Glasgow coma scale
GFAP	Glial fibrillary acidic protein
GO	Gene ontology
GSEA	Gene set enrichment analysis
ISS	Injury severity score
HGF	Hepatocyte growth factor
IL	Interleukin
INR	International normalized ratio
ISS	Injury severity score
JAK-STAT	Janus kinase/signal transducer and activator of transcription
KLK6	Kallikrein-6
LBP	Lipopolysaccharide binding protein
LTA	Lymphotoxin alpha
MAIS	Maximum abbreviated injury scale
MB	Myoglobin
NEFL	Neurofilament light chain
NOS1	Nitric oxide synthase 1
NSE	Neuron-specific enolase
ORA	Over-representation analysis
OSM	Oncostatin M
PCA	Principal component analysis
PEAs	Proximity extension assays
PICU	Pediatric intensive care unit
PRTN3	Proteinase 3
PTT	Partial thromboplastin time
PTX3	Pentraxin 3
RANKL	Receptor activator of NF-κB ligand
RGMA	Repulsive guidance molecule A
sTBI	Severe traumatic brain injury
S100β	S100 calcium-binding proteinβ
TAFA5	TAFA chemokine like family member 5
TIMP1	Tissue inhibitor of metalloproteinases 1
TNF	Tumor necrosis factor
TNFSF	Tumor necrosis factor superfamily
TNNI3	Troponin I3, cardiac type
VWA1	Von Willebrand factor A domain-containing protein 1
VWC2	Von Willebrand factor C domain-containing protein 2 / Brorin
VWF	Von Willebrand factor

Introduction

Severe traumatic brain injury (sTBI) represents a leading cause of mortality in children, accounting for two thirds of deaths at a level 1 pediatric trauma center between 2009 and 2019 [1]. Surviving patients frequently experience persistent neurological deficits, with over half demonstrating functional impairments one-year post-rehabilitation [2, 3]. sTBI results from external mechanical forces that immediately cause permanent or temporary neurological deficits, decreased consciousness, memory loss, and altered mental state [4, 5]. Beyond initial structural damage, cellular function becomes further compromised through secondary injuries including cerebral edema, hemorrhage, and hypoxia [6].

The evolving anatomy of the pediatric brain and skull manifests distinct pathological responses with unique neurological symptoms compared to adults [7–9]. The high plasticity of the pediatric skull and disproportionate head-to-body weight ratio increase children's susceptibility to external forces affecting both brain parenchyma and vasculature. Additionally, reduced myelin abundance and distribution result in differential absorption of traumatic forces, with increased vulnerability in unmyelinated regions. Distinct pathophysiological mechanisms in the pediatric brain, arising from developmental differences compared to the adult brain, cannot be adequately investigated through adult proteomic screening alone. The heterogeneous progression of sTBI, particularly in pediatric populations, presents significant challenges for outcome prediction, necessitating comprehensive approaches to prognosis and pathophysiological investigation [10, 11].

Blood-based injury biomarkers represent a major advancement in sTBI research, utilizing differentially abundant molecules to better characterize injury pathophysiology and disease mechanisms [12–14]. Previous studies have identified biomarkers associated with inflammatory and stress responses, including glial fibrillary acidic protein (GFAP), S100 calcium-binding protein β (S100β), neuron-specific enolase (NSE), and various inflammatory cytokines [12, 15, 16]. However, biomarker utility remains limited by uncertainties regarding TBI specificity and a lack of comprehensive proteomic profiling, with most existing biomarker work focusing on single analytes [17, 18]. Furthermore, no single biomarker has demonstrated accurate TBI outcome prediction to date [19, 20]. Following severe primary injury, increased abundance of neuron- and glial-specific proteins in peripheral blood following blood-brain barrier disruption presents opportunities to develop discrete and comprehensive protein signatures specific to pediatric sTBI [21]. Additionally, cellular damage exacerbated by secondary injuries may be reflected through altered blood protein biomarker levels [18].

Proteomics enables comprehensive investigation and profiling of injury and disease through assessment of circulating proteins [13, 22]. Advanced proximity extension assay (PEA) technology offers high sensitivity and specificity for protein quantification, enabling detection of low-abundance biomarkers with minimal sample

volumes, which is particularly advantageous in pediatric populations [23–25]. When coupled with bioinformatics and machine learning approaches, proteomic signatures provide insights into distinct signaling pathways, enhancing understanding of sTBI-specific mechanisms and pathophysiology [12, 14, 22].

This study aimed to identify plasma proteins unique to pediatric sTBI patients relative to age- and sex-matched healthy controls. Specifically, we sought to: (1) quantify differentially expressed proteins (DEPs) between pediatric sTBI and healthy control cohorts using PEAs; (2) characterize enriched signaling pathways in sTBI; (3) correlate sTBI-specific protein and pathway findings with demographic, clinical, and biochemical variables; and (4) determine protein-protein interactions linked to specific physiological processes.

Methods

Study design and participants

Patients with sTBI were recruited from the Children's Hospital, London Health Sciences Centre (CH-LHSC; London, Ontario, Canada), which is the Regional Pediatric Level 1 Trauma Centre for Southwestern Ontario. CH-LHSC has a catchment area of 190,000 km^2 with a pediatric population of greater than 80,000. We included 20 pediatric patients (age < 18 years) admitted to the Pediatric Intensive Care Unit (PICU) after having sustained a sTBI, defined as a pre-sedation GCS score ≤ 8 and Maximum Abbreviated Injury Scale head (MAIS head) score ≥ 4 [26–30]. Injury data was obtained from our CH-LHSC's trauma registry, which contains detailed injury, clinical and outcome data on severely injured patients as part of the Ontario Trauma Registry's Comprehensive Data Set. Age- and sex-matched healthy controls were recruited from an outpatient clinic. A convenience sample size was employed, as accurate sample size calculations are not feasible for large-scale proteomic studies where effect size and variance are unknown.

Blood collection and processing

Blood samples for proteomic analyses and routine laboratory testing were collected at day 1 of PICU admission while patients received normal saline. Certified nursing personnel collected samples into citrate-containing tubes (Vacutainers; BD Biosciences, Mississauga, Canada) and centrifuged at 1,500×g for 15 min at 4 °C [31, 32]. The upper plasma layer was aliquoted into 250 µL portions and immediately frozen at − 80 °C. Plasma samples remained frozen until analysis, with freeze-thaw cycles avoided.

Proximity extension assays (PEA)

Plasma samples were analyzed using PEA (Olink Explore 1472, Boston, MA) following established protocols [33, 34]. The PEA process involves three steps: (1) antibody binding—antibody pairs tagged with unique DNA oligonucleotides bind specifically to target plasma proteins; (2) proximity-induced hybridization and extension, oligonucleotides in close proximity hybridize and extend via DNA polymerase; and (3) barcode amplification and sequencing, extended DNA barcodes are amplified and analyzed using next-generation sequencing on the NovaSeq Platform (Illumina Inc., San Diego, CA). Results were reported as relative quantification on a $\log_2$ scale of normalized protein expression (NPX) values. Higher NPX values indicate increased protein abundance, with a difference of 1 NPX unit representing a doubling of protein concentration. Rigorous quality control measures for immunoassay performance, detection, and hemolysis ensured all patient and control samples were suitable for analysis. Samples were assessed for quality by automatically identifying outliers in each of the following statistical summaries: Sum of Euclidean distance to other samples, Kolmogorov-Smirnov test statistic, Mean Pearson correlation with other samples, and Hoeffding's D statistic. A sample was classified as an outlier if it failed two or more of the four objective statistical summaries.

Patient demographic data and statistical analysis

Demographic and clinical variables were collected for sTBI patients and included age, weight, sex, etiology, injury severity scores, GCS, pupillary findings, hypotension, surgical interventions and outcomes. Clinical outcome was assessed on the day of PICU discharge, which was different for each patient. The following outcomes were identified: discharged home, discharged to rehabilitation facility, or deceased. Continuous demographic and clinical data are reported as medians with interquartile range (IQR) and compared to healthy control subjects with Mann Whitney U tests. Categorical variables are presented as n (%) and compared to healthy control subjects with chi-square tests.

FDR correction has become the standard approach for large-scale proteomic studies to control for false positives. This method provides an appropriate balance between managing false positive discoveries (approximately 5%) and

limiting stringency for the purpose of an exploratory study compared to more conservative methods like Bonferroni correction which may lead to a high rate of false negatives and loss of statistical power. Our cutoff fold change ≥ 4 is higher than traditional approaches which may limit the detection of more subtle changes. However, given our selected protein panel, this approach ensures robust detection of key biomarkers pertaining to pathophysiological mechanisms by prioritizing large effect sizes. Additionally, a higher fold change cutoff ensures greater reliability for proteins with discriminatory potential between healthy and sTBI plasma samples by reducing false positives.

Machine learning

The Boruta feature selection method iteratively identifies features that are important for predicting the target class. It operates by first creating "shadow" features by shuffling the values of real features. A classifier is then trained on the combined set of real and "shadow" features. The classifier (in this case, the Gradient Boosting Classifier) returns "importance scores" which the Boruta algorithm then uses [35]. Each real feature's importance is compared to the maximally important "shadow" feature. Real features that consistently outperform the "shadow" features are marked as important; features that do not outperform the corresponding "shadow" features are rejected. This procedure is performed iteratively until all features are accepted or rejected, or until a specified number of iterations is achieved. In this study, we ran the Boruta algorithm 100 times and collected the 12 features that were conserved over all 100 runs.

The Gradient Boosting Classifier (GBC) is a form of decision tree classifier which calculates feature importance based on "total impurity reduction" achieved by each feature. In other words, each time a given feature is used to split a node in the decision tree, the GBC algorithm evaluates how much that split reduces "impurity". That is, it evaluates the homogeneity of the resulting groups after a split: if, after splitting, each group contains mostly (or only) samples from a single class, then the split is "pure". Feature importance is the sum of the total increase in purity that each feature contributes across all splits and trees in the ensemble of classifiers.

The performance of the Gradient Boosting Classifier (GBC) was evaluated using 5-fold cross-validation (i.e., an 80/20 train/test split) in conjunction with the Boruta feature selection method. For each fold of the data, a fresh GBC was instantiated, and the Boruta feature selection method was used to identify key features using that fold's training data. Following feature selection, a new GBC was instantiated, fitted on the selected features in the fold's training data and evaluated on the selected features in the fold's test data.

To arrive at just 4 proteins from the original 12, we first trained a new GBC on the 12 selected features and then evaluated the cumulative relative importance in this new classifier. It required only 4 features to account for slightly over 90% of the feature importance, which indicates the predictive power of these features.

To address potential overfitting given our small sample size ($n = 40$ total) and high-dimensional feature space (1,472 proteins), we performed comprehensive validation analyses. Permutation testing was conducted with 100 independent iterations where class labels were randomly shuffled while maintaining the feature structure. For each permutation, a new GBC was trained using the same 5-fold cross-validation procedure with Boruta feature selection. Performance metrics (accuracy and F1 score) were calculated for both the original (correctly labeled) data and each permuted dataset. Statistical significance was assessed by comparing the distribution of permuted performance metrics against the observed performance from correctly labeled data using permutation-based p-values.

Reactome pathway over-representation analysis

Proteins meeting significance criteria (adjusted $P < 0.05$, fold change ≥ 4) were assessed via Reactome pathway ORA. Reactome (package: reactome.db) hierarchically groups known molecular reactions, bindings, and modifications between proteins. Enrichment analysis utilized the clusterProfiler package with identical set size parameters (10–500 proteins) for pathway testing.

Gene ontology (GO) term over-representation analysis (ORA)

Up- and down-regulated proteins significant at adjusted $P < 0.05$ and fold change ≥ 4 in the "sTBI vs Healthy" comparison were mapped to Entrez gene identifiers for GO ORA. Gene Ontologies (package: GO.db v3.20.0) encompass three categories: molecular function (activities of gene products), biological process (biological programs involving multiple molecular activities), and cellular component (subcellular locations of gene products). Enrichment analysis used the clusterProfiler package with minimum and maximum set sizes of 10 and 500 proteins, respectively, required for GO term testing.

Functional analysis (GSEA)

GSEA identified Reactome pathways and GO terms enriched in DEPs. Rather than using filtered significant proteins, all proteins were ordered by significance level and direction of change. Pathway significance was assessed based on disproportionate representation of features at the ordered list extremes.

Pathway associations

GO and Reactome pathways were further analyzed for association with clinical observations, using a graph network approach. The pathways and clinical variables are disjoint sets and thus can be represented as nodes in a bipartite graph. The edges in the graph represent the degree of association between a pathway and a clinical variable. To determine a given pathway's association with a given clinical variable, the given pathway's set of implicated proteins obtained using GO/Reactome ORA was used as an indicator. For each protein, we evaluated two features: the correlation of the protein value with the clinical variable (using Pearson's correlation coefficient ρ), and the protein's relative importance R in differential expression relative to the healthy control group. Taking inspiration from the volcano plot, which presents impact (log2 fold change) and significance (-log10(adjusted p-value)) in a two-dimensional plane, we can combine these two features into a single measure of the protein's relative importance:

$$\mathrm{R} = \sqrt{\left(\log_2\left(\text{fold change}\right)\right)^2 + \left(-log_{10}\left(\text{adjusted p-value}\right)\right)^2}$$

Then, for each protein the weight w for its association with a clinical variable is given by

$$w = \rho\, R$$

When the Pearson's ρ was significant for a given protein/clinical variable pair (with a Pearson's p-value < 0.05), we added an edge to the graph network, representing a connection between the given pathway (via the protein) and the clinical variable (i.e., the nodes in the graph). Comparisons that were not significant were not included. By summing the edge weights over pathway/clinical variable pairs, we obtained a representation of the strength of association between the pathway and the clinical variable.

Protein-protein interaction

Protein-protein interactions were analyzed using STRING (https://string-db.org/) to identify functional networks among DEPs. The top 50 DEPs, ranked by FDR-adjusted P-value, were uploaded to the STRING database. Analysis parameters included: full STRING network selection, high confidence score threshold (0.7), first shell set to 1 with no second shell interactions. Protein clustering employed k-means clustering with $k = 5$ to identify optimal functional clusters within the interaction network.

Results

Patient demographics and clinical characteristics

We examined the plasma proteomes of 20 individuals with sTBI and 20 age- and sex-matched healthy controls, with an average age of 13 and a 10:10 male:female split across both cohorts. Demographic and clinical data are presented in Fig. 1A. Admission computed tomography (CT) abnormalities and laboratory biochemistry values are presented in Supplemental Table 1. Principal component analysis (PCA) of proteomics data revealed distinct cohort separation, with healthy controls demonstrating tighter clustering while sTBI patients displayed greater variability, indicating notable differences in protein abundance between groups (Fig. 1B). Healthy controls demonstrate tighter clustering across principal component analysis based on NPX values, while sTBI patients show greater variability demonstrated in a correlation heatmap (Fig. 1C).

Differentially expressed proteins

Comparison between sTBI patients and healthy controls using significance thresholds of FDR-adjusted $P < 0.05$ and fold change ≥ 4 identified (Fig. 2A). Figure 2B illustrates protein expression levels, with red and blue indicating upregulation and downregulation, respectively. sTBI patient samples displayed greater protein upregulation compared to healthy controls, with detailed fold change, effect size, P-values, and adjusted P-values shown in Fig. 2C.

GFAP and TNFSF11 demonstrated the greatest upregulation and downregulation, respectively (Fig. 2A). Additional notably upregulated proteins included IL-6, IL1RL1, VWA1, and NEFL, while TNFSF11 and VWC2 were downregulated. Additional DEPs selected based on lowest adjusted P-values are depicted in Fig. 3. Using decision tree methods and Boruta feature selection, four proteins (VWA1, TNFSF11, VWC2, and IL-6) were sufficient to differentiate sTBI patients from healthy controls (Supplemental Figs. 2 and 3).

The GBC model was validated using 5-fold cross-validation in conjunction with Boruta feature selection. Across all folds, the number of Boruta-selected features ranged from

A

Admission variables	Statistics
Age (years), median (IQR)	14.5 (7.3)
Weight (Kg), median (IQR)	59 (32.5)
Male, n (%)	10 (50%)
Etiology- All Blunt Mechanism of Injury	
MVC, n (%)	15 (75%)
Fall, n (%)	1 (5%)
Intentional, n (%)	1 (5%)
Other, n (%)	3 (15%)
Injury severity score, median (IQR)	38 (12.8)
Injury profile, median (IQR)	
MAIS HEAD	5 (0)
MAIS NECK	1 (1)
MAIS Face	1 (1)
MAIS Thorax	3 (1)
MAIS Abdomen	2 (0)
MAIS Spine	2 (0.8)
MAIS Upper extremity	2 (0)
MAIS Lower extremity	2 (1)
MAIS External	1 (0)
MAIS Other	3 (0)
Pre-sedation GCS, median (IQR)	3 (3)
Pre-sedation motor GCS, median (IQR)	1 (1)
Bilateral fixed pupils, n (%)	9 (45%)
Hypotensive episode, n (%)	10 (50%)
Emergent surgical intervention, n (%)	2 (10%)
Outcomes	
Mortality, n (%)	6 (30%)
Ventilator free days, median (IQR)	14 (28)
Outcomes For survivors (n=14)	
Hospital - LOS (days) median (IQR)	29 (70)
PCCU - LOS (days) median (IQR)	12.5 (8.5)
Discharged to:	
Rehabilitation facility, n (%)	9 (45%)
Home, n (%)	5 (25%)

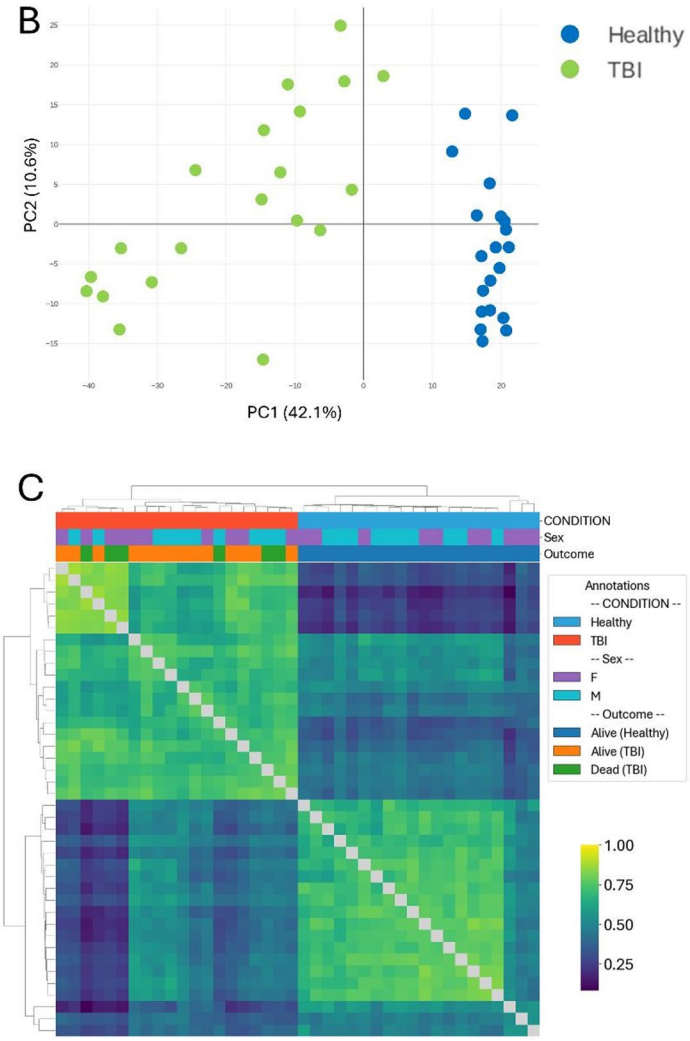

Fig. 1 Pediatric sTBI patient characteristics and plasma proteome overview. **A** Demographic and clinical data for pediatric sTBI patients ($n=20$) and healthy controls ($n=20$). **B** Principal component analysis (PCA) scatterplot of the first two principal components from normalized proteomic data. Colors correspond to study cohorts: sTBI patients (green) and healthy controls (blue). Healthy controls demonstrate tighter clustering while sTBI patients show greater variability, indicating notable differences in protein abundance between groups. **C** Correlation heatmap showing between-sample pairwise Pearson correlations of normalized proteomic data. Individual samples are displayed along both axes, with correlation degree indicated by color intensity (yellow: higher correlation; purple: lower correlation). Hierarchical clustering (Euclidean distance) is shown by dendrograms above and left of the heatmap, with relevant sample annotations

13 to 27, with 12 features conserved across all folds. The resulting GBC achieved perfect classification performance (prediction accuracy = 1.0, F1 score = 1.0), consistent with the clear proteomic separation between sTBI patients and healthy controls observed across all analytical approaches.

Permutation testing with 100 random label shuffles demonstrated that the model's perfect classification performance significantly exceeded chance. The regular model achieved mean accuracy of 1.0000 and mean F1 score of 1.0000, whereas permuted models (with shuffled labels) achieved mean accuracy of 0.4696 ± 0.1129 and mean F1 score of 0.4545 ± 0.1142 (both $p<0.0001$). These results confirm that the observed perfect classification is statistically significant and not due to overfitting or chance.

Functional analysis and clinical correlation

Functional enrichment analysis was performed to identify overrepresented GO terms and Reactome pathways that were enriched in DEPs. At a statistical threshold of FDR-adjusted $P<0.05$, there were four enriched GO terms, namely "Cytokine activity", "Receptor ligand activity", "Signaling receptor activator activity" and "Cytokine receptor binding" (Fig. 4). Additional GO pathways are presented in Supplemental Table 2. Similarly, three Reactome pathways were significantly enriched in proteins associated with the "TBI vs. Healthy" contrast, namely "Interleukin-10 signaling", "Protein localization", and "Interleukin-4 and

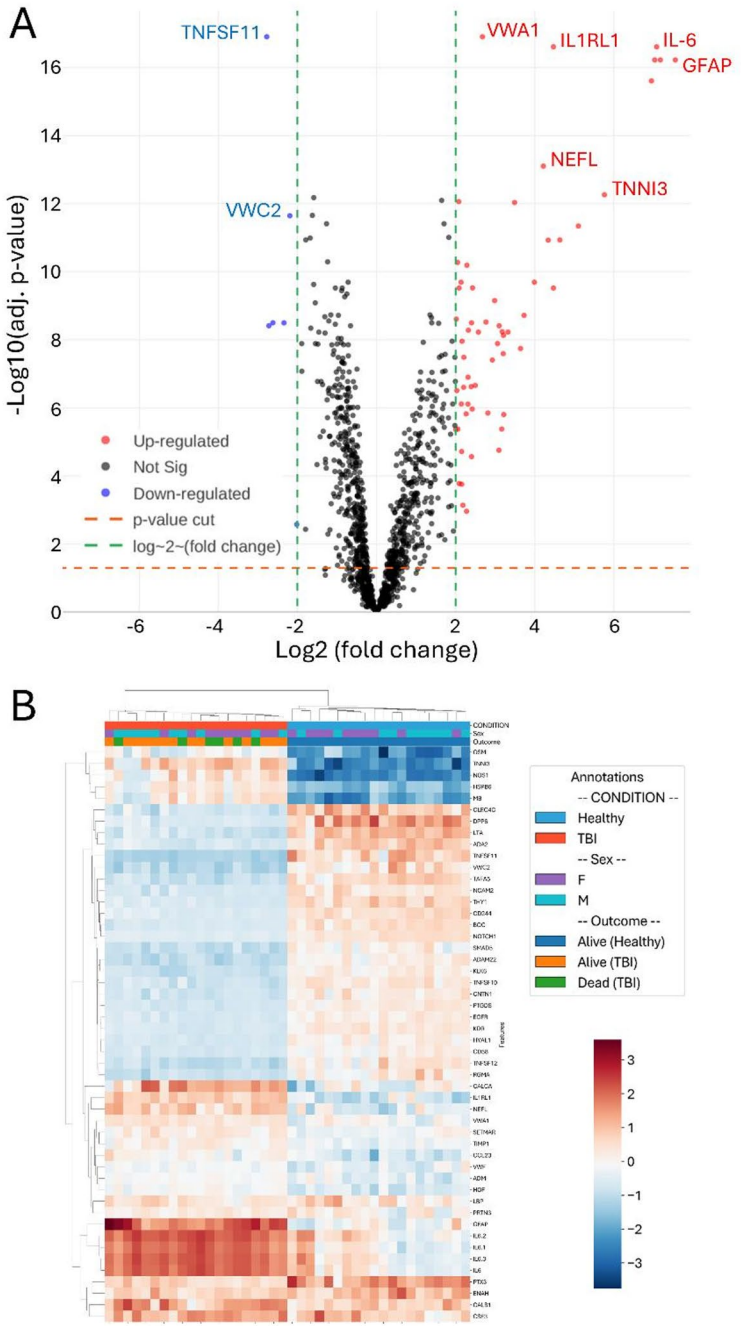

C

Protein	FC	effect	P.Value	adj.P.Val
VWA1	6.399	2.678	1.58e-20	1.25e-17
TNFSF11	-6.853	-2.777	1.7e-20	1.25e-17
IL1RL1	22.223	4.474	5.84e-20	2.47e-17
IL-6	135.63	7.084	6.7e-20	2.47e-17
IL-6	144.539	7.175	2.31e-19	5.99e-17
GFAP	187.971	7.554	2.79e-19	5.99e-17
IL-6	131.111	7.035	2.85e-19	5.99e-17
IL-6	123.832	6.952	1.34e-18	2.47e-16
NEFL	18.606	4.218	4.81e-16	7.87e-14
TNNI3	54.321	5.763	3.72e-15	5.47e-13
ADAM22	-3.005	-1.587	4.96e-15	6.64e-13
ADM	3.132	1.647	6.54e-15	8.02e-13
LBP	4.226	2.079	7.67e-15	8.69e-13
HSPB6	11.238	3.49	8.79e-15	9.24e-13
TNFSF12	-3.078	-1.622	2.25e-14	2.21e-12
VWC2	-4.571	-2.193	2.46e-14	2.26e-12
PTX3	3.264	1.707	4.59e-14	3.89e-12
KLK6	-2.401	-1.264	4.76e-14	3.89e-12
CALCA	34.414	5.105	5.85e-14	4.53e-12
HGF	3.548	1.827	1.33e-13	9.78e-12
TAFA5	-3.201	-1.678	1.45e-13	1.02e-11
LTA	-3.455	-1.789	1.78e-13	1.16e-11
NOS1	24.852	4.635	1.81e-13	1.16e-11
CALB1	20.262	4.341	1.92e-13	1.18e-11
RGMA	-2.356	-1.236	8.68e-13	5.11e-11
PRTN3	4.139	2.049	9.4e-13	5.32e-11
SETMAR	4.874	2.285	1.18e-12	6.44e-11
MB	15.908	3.992	3.93e-12	2.03e-10
TIMP1	4.398	2.137	4.09e-12	2.03e-10
CLEC4C	-3.011	-1.59	4.96e-12	2.36e-10
ENAH	5.383	2.428	6.45e-12	2.97e-10
CCL23	4.25	2.087	6.86e-12	3.0e-10
CSF3	22.212	4.473	6.98e-12	3.0e-10
CNTN1	-2.059	-1.042	7.33e-12	3.0e-10
OSM	7.921	2.986	1.91e-11	7.04e-10
DPP6	-2.928	-1.55	2.28e-11	8.17e-10
TNFSF10	-2.227	-1.155	5.27e-11	1.85e-9
VWF	2.552	1.352	5.4e-11	1.85e-9
PLA2G2A	13.274	3.73	5.83e-11	1.91e-9
SMAD5	-2.477	-1.308	6.54e-11	2.09e-9
PPP3R1	2.621	1.39	7.11e-11	2.23e-9
TNFSF14	4.052	2.019	8.04e-11	2.47e-9
ADA2	-2.31	-1.208	9.27e-11	2.79e-9
CCL7	6.806	2.767	1.02e-10	3.0e-9
CRH	-6.147	-2.62	1.11e-10	3.15e-9
GDF15	5.285	2.402	1.13e-10	3.15e-9
CTSL	2.632	1.396	1.14e-10	3.15e-9
OMG	-5.065	-2.341	1.16e-10	3.16e-9
ANGPTL4	2.971	1.571	1.22e-10	3.27e-9
THY1	-2.06	-1.043	1.33e-10	3.48e-9

Fig. 2 Differentially expressed proteins in pediatric sTBI plasma. **A** Volcano plot displaying significance (-log$_{10}$ transformed *P*-values) versus magnitude (log$_2$ fold change) for all analyzed proteins. Proteins with significantly different expression levels are represented as red dots (upregulated) or blue dots (downregulated) in sTBI patients compared to healthy controls. Non-significant proteins are shown as black dots (representative subsample). Vertical green lines represent fold change thresholds (≥4-fold), and horizontal orange line represents significance threshold (FDR-adjusted $P<0.05$). **B** Heatmap showing relative protein intensity per sample compared to average levels across all samples. Individual proteins are displayed on the Y-axis and samples on the X-axis. Red and blue cells correspond to higher and lower protein levels, respectively. Analysis includes up to 1,000 features and 1,000 samples (randomly selected when numbers exceed limits). **C** Table displaying significance values and fold changes for 65 differentially expressed plasma proteins meeting significance criteria. Red text indicates upregulated proteins, and blue text indicates downregulated proteins in sTBI patients versus controls. Fold change represents the ratio of mean protein expression in sTBI vs. controls, and effect size refers to Cohen's d, a standardized measure of the magnitude of difference between groups

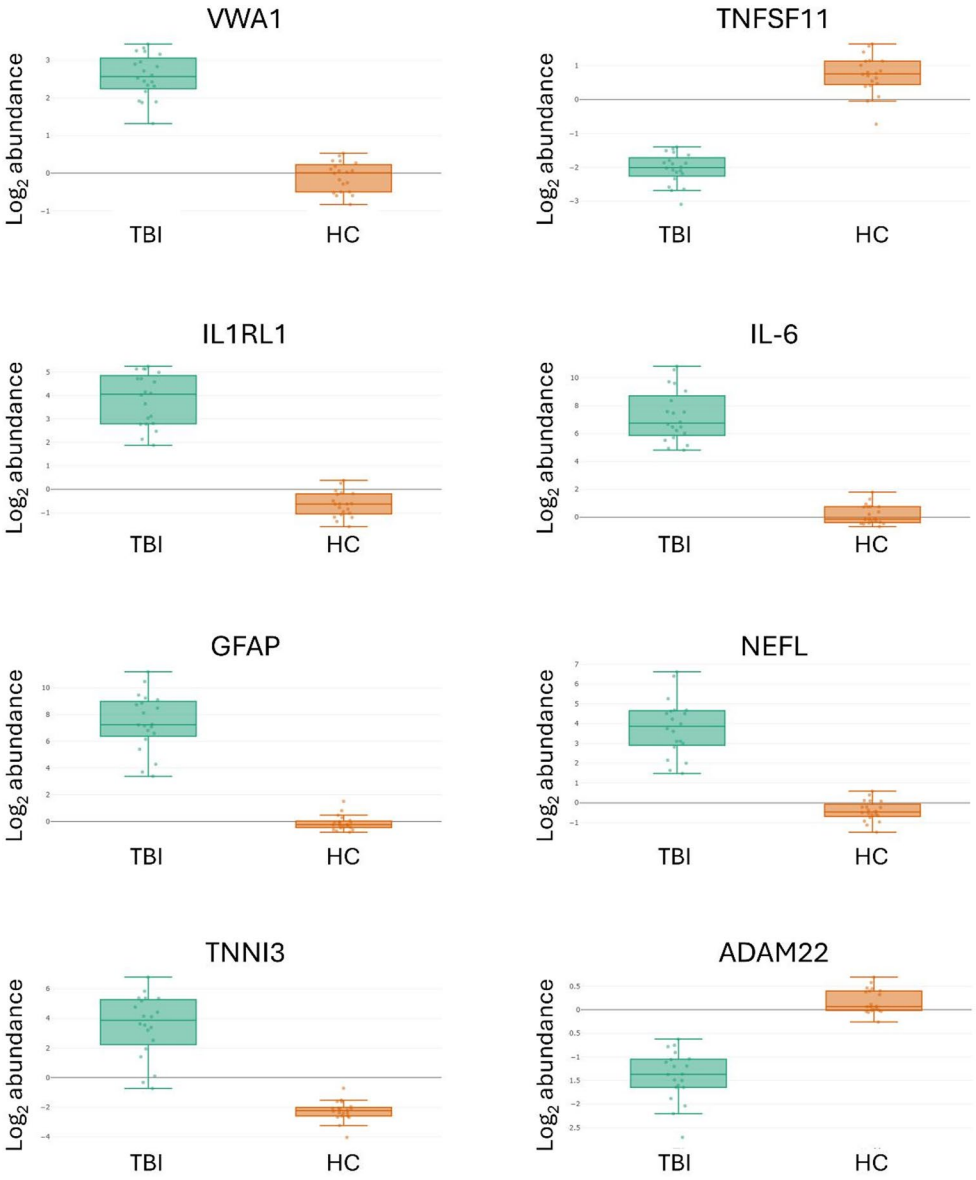

Fig. 3 Expression profiles of top differentially expressed proteins. Boxplots display the eight most significantly differentially expressed proteins in pediatric sTBI patients versus healthy controls, selected based on lowest FDR-adjusted *P*-values. Y-axis represents $\log_2$-transformed normalized protein expression (NPX) values to facilitate visualization. Relative expression values are non-descriptive and do not correspond to absolute protein concentrations. Individual data points represent individual patient samples, with box plots showing median, quartiles, and range

Interleukin-13 signaling" (Fig. 4). A comprehensive list of statistically significant Reactome pathways is presented in Supplemental Table 3. There were no significantly enriched pathways in the "TBI (Dead) vs. TBI (Alive)" contrast given that no differentially expressed proteins were identified.

Relationships between clinical features of sTBI and enriched biological pathways, using pathway-associated proteins as indicators, are shown in Fig. 4B. Associations between protein pathways and clinical variables were determined using a combined measure of a protein's correlation with a particular variable and its differential expression within a specific pathway. All pathways demonstrated positive correlations with injury severity score (ISS), most notably "Signaling Receptor Activator Activity," "Receptor Ligand Activity," and "Cytokine Activity." Glucose, international normalized ratio (INR), and partial thromboplastin time (PTT) values showed positive correlations with all pathways, except "Protein Localization" for glucose and INR. Conversely, all pathways demonstrated negative correlations with vault skull fracture, albumin, arterial pH, and base excess, except for "Protein Localization" for arterial pH. Motor vehicle crash injuries predominantly showed positive pathway correlations, while injuries classified as "other" were negatively correlated. Weak but positive associations were observed between all pathways and GCS $\leq$ 6, indicating elevated pathway activity with decreased consciousness.

Gene set enrichment analysis

GSEA was used to assess the strength and direction of activity in enriched GO term/Reactome pathways (Fig. 5).

A

GO term ORA	S	N	S/N (%)	OR	Z-score	P	P (adj.)
Cytokine activity	17	109	15.6	5.74	1.44	4.25e-7	0.000813
Receptor ligand activity	20	205	9.76	3.36	1.12	6.75e-5	0.0463
Signaling receptor activator activity	20	208	9.62	3.3	1.11	8.38e-5	0.0463
Cytokine receptor binding	14	114	12.3	4.04	1.12	9.68e-5	0.0463
Reactome pathway ORA	**S**	**N**	**S/N (%)**	**OR**	**Z-score**	**P**	**P (adj.)**
IL-10 signaling	8	30	26.7	8.68	1.46	3.21e-5	0.00398
Protein localization	5	13	38.5	14.2	1.39	0.000168	0.0104
IL-4 and IL-13 signaling	8	45	17.8	5.09	1.19	0.000689	0.0285

B

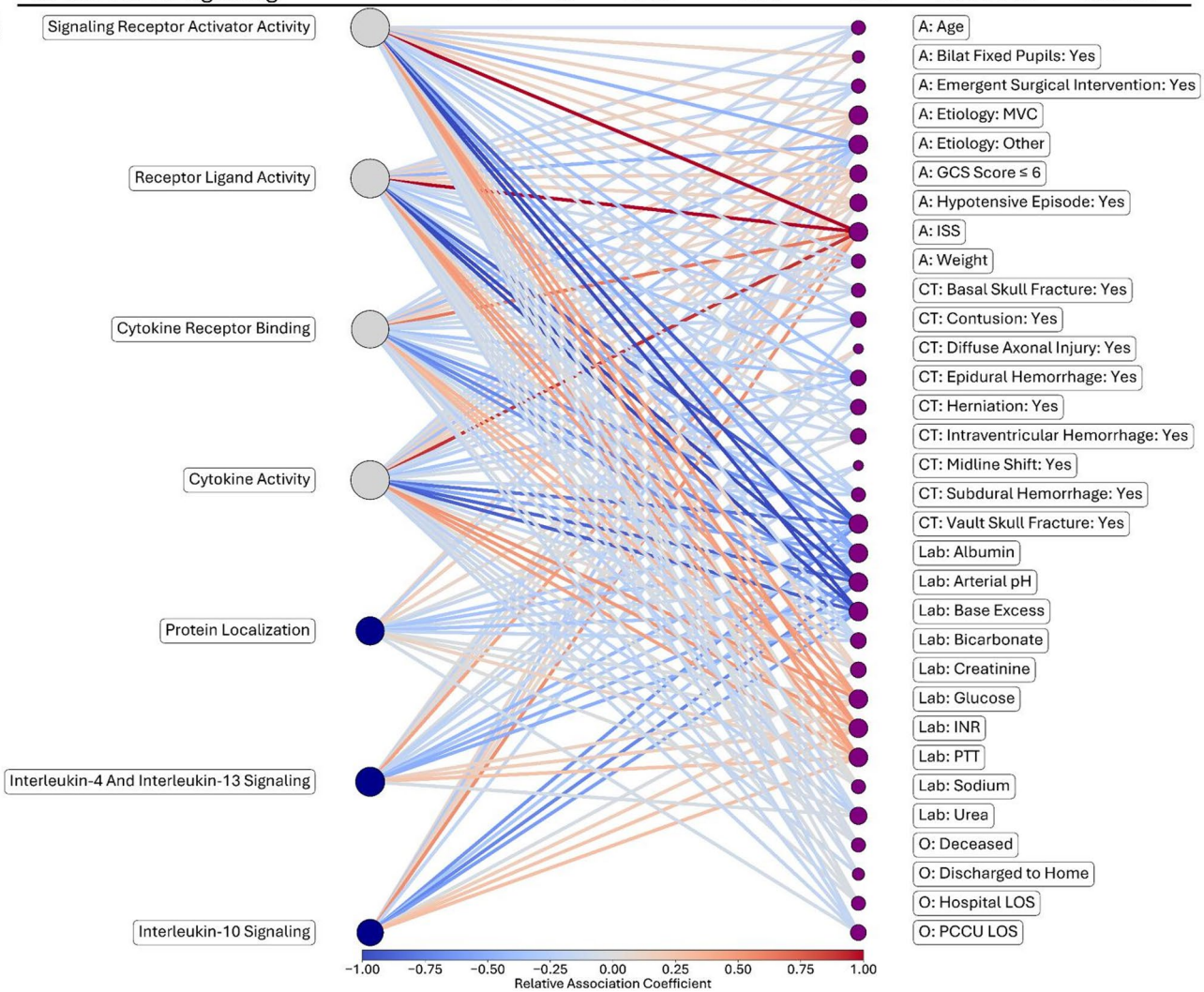

Fig. 4 Functional pathway enrichment and clinical correlations. **A** Over-representation analysis (ORA) identifying significantly enriched Gene Ontology (GO) terms and Reactome pathways in differentially expressed proteins. At FDR-adjusted $P<0.05$, four GO terms ("Cytokine activity," "Receptor ligand activity," "Signaling receptor activator activity," "Cytokine receptor binding") and three Reactome pathways ("Interleukin-10 signaling," "Protein localization," "Interleukin-4 and Interleukin-13 signaling") were significantly enriched in the sTBI versus healthy comparison. S = number of differentially expressed proteins from our study found in the pathway; N = total number of proteins in the pathway; S/N = ratio representing the proportion of pathway proteins detected in our dataset; OR = odds ratio, indicating the strength of enrichment (values > 1 indicate over-representation); q = FDR-adjusted *p*-value for enrichment significance. **B** Bipartite network showing pathway-clinical variable associations calculated using weighted correlations between pathway proteins and clinical variables. Pathways are displayed on the left, clinical features on the right. Edge thickness indicates association strength, while edge color represents direction and magnitude of association (red: positive correlation; blue: negative correlation). Clinical variables include injury severity score (ISS), Glasgow Coma Scale (GCS), biochemical parameters, and injury characteristics. Node sizes are proportional to the number of proteins in the pathway (larger nodes = more proteins). Pathway node color indicates biological database source: gray (Gene Ontology) and blue (Reactome)

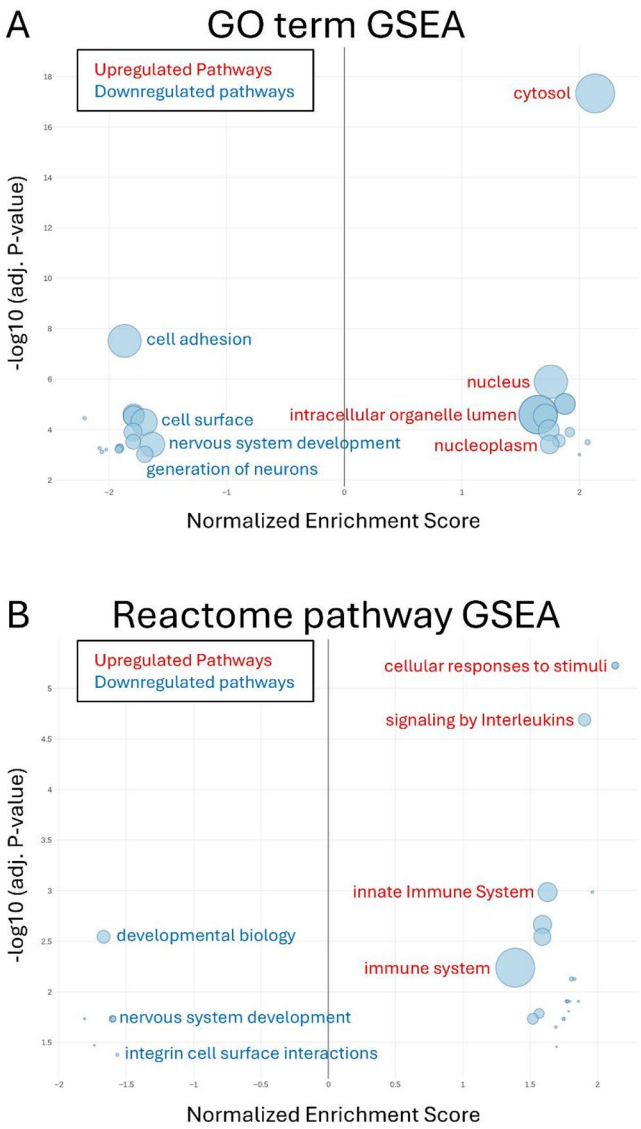

Fig. 5 Gene set enrichment analysis of functional pathways. **A** Gene Ontology (GO) term enrichment analysis identified 178 significantly enriched terms. Terms related to cytosol, nucleus, intracellular organelle lumen, and nucleoplasm were over-represented in upregulated proteins (red text). Terms related to cell adhesion, cell surface, and nervous system were over-represented in downregulated proteins (blue text). Dot size represents gene set size, while color intensity indicates normalized enrichment score. **B** Reactome pathway enrichment analysis identified 29 significantly enriched pathways. Pathways related to cellular responses to stimuli, interleukin signaling, and immune system function were over-represented in upregulated proteins (red text). Pathways related to developmental biology, nervous system development, and integrin cell surface interactions were over-represented in downregulated proteins (blue text)

A total of 178 GO terms and 29 Reactome pathways were significantly enriched. GO terms related to cytosol, nucleus, intracellular organelle lumen, and nucleoplasm were over-represented in up-regulated proteins **(**Fig. 5A**).** Conversely, terms related to cell adhesion, cell surface and the nervous system were over-represented in down-regulated proteins. Reactome pathways related to cellular responses to stimuli, interleukin signaling and the immune system were over-represented in up-regulated proteins, whereas pathways related to developmental biology, nervous system development and integrin cell surface interactions were over-represented in down-regulated proteins **(**Fig. 5B**).**

Protein-protein interactions

STRING protein-protein interactions were identified amongst the top 50 DEPs according to FDR *p*-value (Fig. 6). IL-6 was identified as the central node, with the subcluster "Opsonization" (12 proteins) largely dominating the interaction network. "TNF Family" (5 proteins), "Neuronal/Astrocytic Injury" (CALB1, GFAP, and NEFL), "Amidation" (CALCA, ADM, and CRH), and "Muscle Pathophysiology" (MB, NOS1, and TNNI3) emerged as separate clusters.

Discussion

In this study, we analyzed the plasma proteome of pediatric patients with sTBI compared to age- and sex-matched healthy controls. At a threshold of FDR-adjusted $P<0.05$ and fold change$\geq$4, we identified 65 DEPs, with four features sufficient to differentiate between healthy and injured cohorts. Functional enrichment analysis using GSEA identified 178 GO terms and 29 Reactome pathways significantly enriched in DEPs. Pathway-clinical variable associations were calculated using weighted correlations between pathway proteins and clinical variables, revealing pathways correlating with clinical biochemistry, assessments, and injury etiology. IL-6 was identified as a central hub protein.

Clinical data revealed a median ISS of 38 and a pre-sedation GCS of 3, two strong indicators of severe trauma [36]. This cohort largely consists of patients injured in motor vehicle crashes (75%), which are a common cause of sTBI [7]. Of the 20 sTBI patients, 14 patients survived with 9 transferred to a chronic rehabilitation hospital and 5 discharged to their home.

Proteomic signatures and neuroinflammatory response

We used PEA for high-throughput protein quantification [37] and identified IL-6 and GFAP as the most upregulated proteins in sTBI versus healthy controls, consistent with previous TBI associations [38]. The proteomic signature suggests coordinated inflammatory and structural damage responses. IL-6 upregulation triggers acute phase responses and lymphocyte activation [39], accompanied by

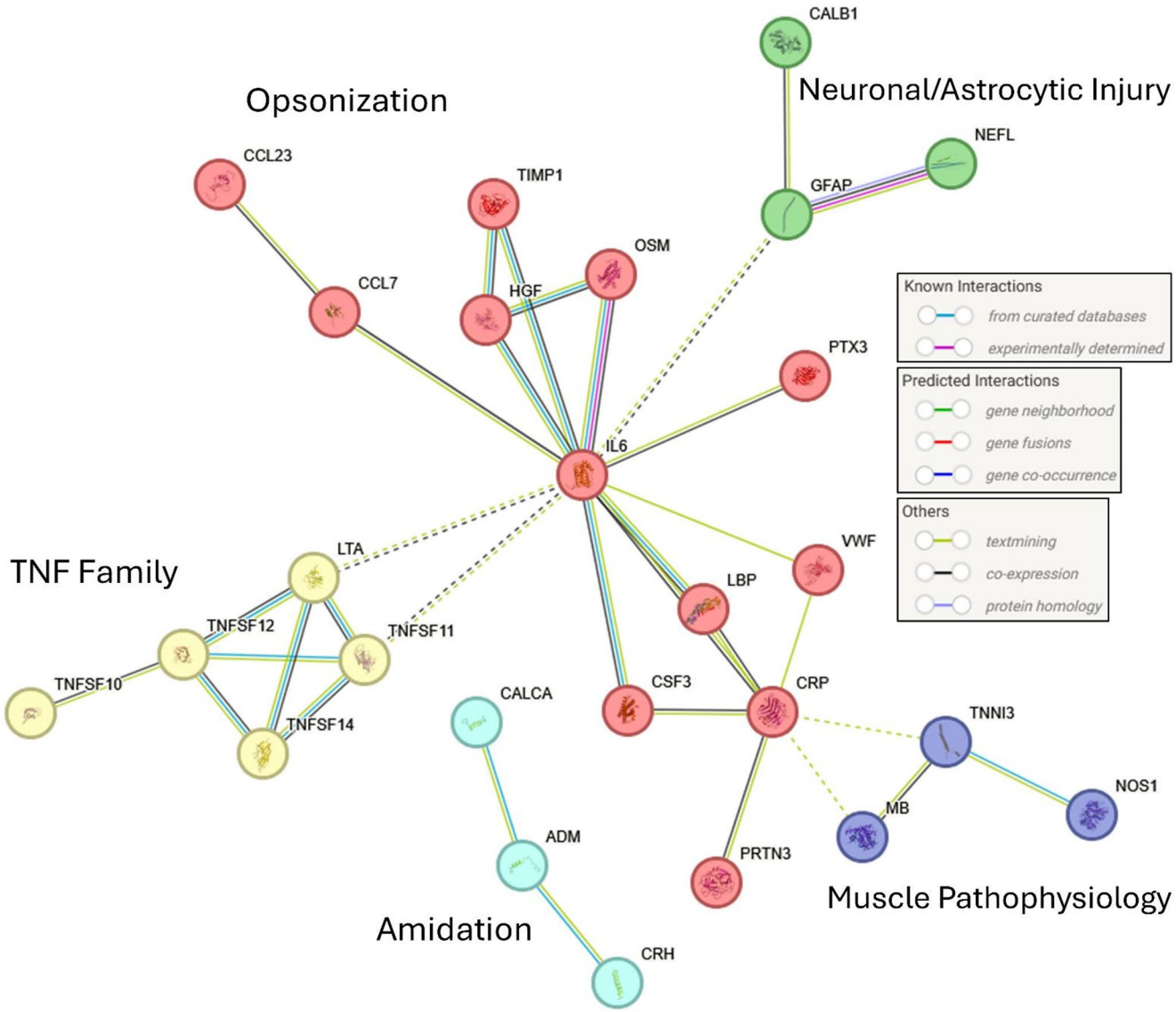

Fig. 6 Protein-protein interaction network of differentially expressed proteins. STRING network analysis of the top 50 differentially expressed proteins (ranked by FDR-adjusted *P*-value) reveals functional protein clusters and interactions. IL-6 serves as the central hub connecting multiple inflammatory, immune response, and signaling molecules including CCL7, TIMP1, OSM, HGF, PTX3, VWF, CRP, LBP, and CSF3. Distinct functional subclusters are identified: [1] Opsonization cluster containing CCL23, CCL7, TIMP1, and OSM; [2] TNF family cluster with TNFSF10, TNFSF11, TNFSF12, TNFSF14, and LTA involved in immune modulation; [3] Amidation cluster including CALCA, ADM, and CRH; [4] Multifaceted sTBI responses cluster with MB, NOS1, and TNNI3; and [5] Neuronal/glial injury cluster containing CALB1, GFAP, and NEFL reflecting neuronal and astrocytic damage, neuronal protection, tissue repair, and inflammation. Network analysis used high confidence interactions (score ≥ 0.7) with k-means clustering (k = 5). Solid lines indicate direct evidence interactions; dotted lines indicate indirect/predicted interactions. Edge colours indicate the source where an interaction is determined, as shown in the figure legend. STRING derives confidence based on the direct evidence available for an interaction. Interactions determined from curated databases and experiments represent high confidence interactions due to direct evidence. Lower confidence interactions are derived from predicted associations through indirect evidence, such as gene neighbourhood and co-occurrence

increased IL1RL1 (an IL-33 receptor and adaptive immune marker) [40], and decreased TNFSF11 (suggesting reduced RANKL-mediated immune signaling) [41]. Additionally, upregulation of GFAP (an intermediate filament protein of astrocytes) [21, 42] and NEFL (a neurofilament involved in axonal growth and stability) [43] in sTBI samples compared to healthy controls suggests structural impairment and cellular damage due to elevated plasma abundance.

Contrary to prior studies linking IL-6 and GFAP to poor TBI outcomes [44, 45], we found no significant protein differences between deceased (n = 6) and surviving (n = 14) sTBI patients. The small sample size and uneven group

distribution may have limited our ability to detect outcome-associated protein changes.

Pathway enrichment and mechanistic insights

Neuroinflammation following sTBI initially promotes repair but contributes to secondary injury propagation and neurodegeneration [46]. Our study identified significantly enriched pathways suggesting enhanced inflammatory responses, specifically "Cytokine activity," "Cytokine receptor binding," and "IL-4 and IL-13 signaling." Increased IL-4 and IL-13 activity exacerbates inflammatory responses by promoting the JAK-STAT pathway [47, 48]. Reactome pathways including "Signaling by interleukins," "Innate immune system," and "Immune system" indicate immune activation and infection response, common sTBI sequelae [27]. Conversely, "IL-10 signaling" represents a potent anti-inflammatory pathway, suggesting physiological counter regulation attempting to control excessive neuroinflammation [49].

Clinical correlations and biomarker potential

Altered pathways demonstrated both positive and negative associations with clinical variables. Strong positive correlations existed between ISS and Reactome pathways, particularly those pertaining to inflammatory activation and receptor-ligand activity. Literature suggests correlations between ISS and increased inflammatory cytokine production, and that cytokine abundance assessment may improve TBI outcome and progression prognosis [50]. Positive but weaker correlations were observed with GCS scores, potentially due to limited GCS variation among sTBI patients. These correlations likely reflect enhanced neuroinflammatory pathways in sTBI contexts, as indicated by decreased consciousness [50]. These pathways also demonstrated positive correlations with glucose, INR, and PTT. Hyperglycemia in TBI is commonly associated with elevated cytokine production and endothelial dysfunction [51]. Additionally, positive correlations with INR and PTT indicate coagulopathy [52], illustrating consequences of disturbed endothelial cell functions with elevated inflammatory cytokine production.

Strong negative correlations occurred with arterial pH and base excess, particularly through receptor-ligand and cytokine signaling. Our data indicates generally decreased pH (median 7.29) and negative base excess (median − 5.5), indicating blood acid surplus. pH decrease reportedly decreases receptor-ligand interactions by affecting protonation states, thus altering binding affinity [53]. In acidic pH patients, this may reflect observed negative pathway correlations. Strong negative correlations were also observed in patients with vault skull fractures. Patients with skull fractures often experience direct damage to signaling pathway cells, disrupting normal ligand-receptor interaction production and activity, reducing signaling [54].

Decision tree analysis identified four key proteins differentiating healthy and sTBI cohorts. VWA1 demonstrated the highest discriminatory importance and functions in blood-brain barrier maintenance and vascular stability through extracellular matrix stabilization by facilitating structural bridging (e.g. collagen and proteoglycan binding) [55]. VWA1 upregulation likely reflects compensatory mechanisms attempting to restore vascular integrity following blood-brain barrier breakdown. VWC2 downregulation indicates impaired neurogenesis, as this protein facilitates neural development and synaptic plasticity by inhibiting bone morphogenetic protein 2 (BMP-2), which is critical for nervous system development [56]. In pediatric populations, VWC2 suppression may compromise ongoing brain maturation processes, including synaptogenesis and myelination, potentially contributing to long-term cognitive and developmental deficits observed following childhood sTBI. The prominence of IL-6 and TNFSF11 among discriminatory features underscores the central role of neuroinflammatory dysregulation in sTBI pathophysiology [39, 57]. IL-6 elevation reflects activated microglia and astrocytes releasing pro-inflammatory mediators that can exacerbate secondary brain injury through oxidative stress and excitotoxicity. Conversely, TNFSF11 downregulation may indicate disrupted immune regulatory mechanisms through diminished RANK ligand signaling, normally responsible for resolving inflammation and promoting tissue repair, suggesting a shift toward chronic neuroinflammation that impedes recovery.

While our machine learning model achieved perfect classification performance (accuracy = 1.0, F1 = 1.0), comprehensive validation analyses including permutation testing confirmed this result is statistically significant and not due to chance ($p < 0.0001$ for both metrics). The substantial biological separation between sTBI patients and healthy controls—evidenced by clear PCA clustering, distinct volcano plot patterns, and enriched pathway signatures—likely explains the high discriminatory accuracy. However, we emphasize that this machine learning analysis serves as supporting evidence consistent with our primary statistical and pathway analyses rather than as a standalone predictive model.

Brain endothelial dysfunction and vascular disruption

Systemic inflammation in sTBI causes endothelial activation and barrier dysfunction, propagating inflammation and cerebral edema through increased permeability [51]. Our analysis reveals upregulation of factors involved in endothelial

dysfunction (IL-6, PRTN3) and vasodilators (CALCA, ADM) that may disrupt barrier integrity. Coagulation factors were also upregulated (VWA1, VWF), likely indicating endothelial activation preventing bleeding [58]. GSEA reveals downregulation of "cell adhesion," "cell surface," and "integrin cell surface interaction," indicating vascular disruption and altered receptor-ligand interactions among other cellular damages. Altered GO/Reactome pathways such as "signaling receptor activator activity" and "receptor ligand activity" may contribute to endothelial dysfunction through neuroinflammation. These pathways positively correlate with glucose levels, supporting hyperglycemia's role in endothelial and vascular pathological changes [51]. Furthermore, positive correlations with INR and PTT reflect coagulation dysfunction, where the endothelium plays a key modulatory role [59].

Neuronal and astrocytic disruption

Proteomic analyses reveal significant neuronal and glial cell disruption in sTBI patients. NEFL upregulation reflects axonal damage, as neurofilaments maintain axonal diameter and optimize conduction velocity [60]. GFAP upregulation indicates both astrocytic structural damage and reactive astrogliosis, with the latter being a complex process involving astrocytic hypertrophy, proliferation, and scar formation that can be either neuroprotective or detrimental to recovery [42]. The concurrent elevation of neuronal and astrocytic markers demonstrates the multi-cellular nature of sTBI pathology, where primary mechanical forces trigger cascading damage across cell types. Brain homeostasis mediated by neuronal-astrocytic interactions is disrupted after sTBI and is especially problematic in pediatric populations where brain development requires coordinated cellular function [9]. These findings support multi-protein panels for comprehensively assessing brain tissue damage and guiding therapeutic interventions targeting specific cellular pathways.

Enrichment analysis of GO terms/Reactome pathways revealed decreased "nervous system development," "generation of neurons," and "developmental biology." Downregulation of ADAM22, a brain-specific cell surface protein crucial for synaptic maturation and Schwann cell myelination [61], aligns with decreased "cell surface" pathway activity. We also observed VWC2/brorin downregulation, which plays roles in neural development and function [56]. Further downregulation of proteins involved in nervous system function and structure (RGMA, TAFA5, KLK6) indicates cellular disruption. Pathway analysis suggests notable decreases in developmental and neural biology, reflected in decreased corticotropin-releasing hormone (CRH) abundance, a stress response hormone involved in neural development [62].

Protein-protein interaction networks

STRING analysis revealed distinct functional subclusters among the top 50 DEPs, with IL-6 emerging as the central hub reflecting its critical role in coordinating neuroinflammatory responses. This network architecture demonstrates the interconnected nature of sTBI pathophysiology, where inflammatory, structural, and metabolic disruptions cascade through multiple biological systems.

The opsonization cluster represents the largest network component, reflecting massive activation of innate immune responses following sTBI. This process involves tagging of cellular debris and foreign particles by opsonins for phagocytic clearance [63]. Key opsonins identified include lipopolysaccharide binding protein (LBP), C-reactive protein (CRP), and pentraxin 3 (PTX3), which directly facilitate recognition and elimination of damaged tissue components [64–66]. Downstream amplification occurs through pleiotropic cytokines including IL-6, oncostatin M (OSM), and hepatocyte growth factor (HGF), which coordinate both local and systemic inflammatory responses [39, 67, 68]. This network includes critical immune modulators: chemokines CCL23 and CCL7 facilitate leukocyte recruitment to injury sites [69], while CSF3 regulates immune cell production and mobilization from bone marrow [70]. Von Willebrand factor (vWF) promotes leukocyte extravasation across the compromised blood-brain barrier [71] enabling peripheral immune cell infiltration that can exacerbate secondary brain injury. The presence of TIMP1 and PRTN3 indicates activation of neutrophil extracellular trap formation (NETosis) and degranulation, respectively [72, 73]. While these mechanisms serve to eliminate pathogens and debris, excessive activation can damage healthy brain tissue through release of proteases and reactive oxygen species, contributing to secondary injury progression.

The TNF family subcluster reveals complex immune regulatory disruption, characterized by downregulation of lymphotoxin alpha (LTA) and most TNF superfamily proteins, with TNFSF14 as a notable exception. This pattern suggests an attempted shift toward anti-inflammatory states following the initial pro-inflammatory burst [57]. However, this suppression may impair normal immune resolution mechanisms, potentially contributing to delayed recovery and increased susceptibility to secondary complications. The selective preservation of TNFSF14 expression may represent a compensatory mechanism attempting to maintain minimal immune surveillance capacity.

The Neuronal/astrocytic injury cluster suggests cellular damage through release of intracellular structural proteins into peripheral circulation. GFAP and NEFL elevation reflects astrocytic and axonal damage, respectively, serving as established biomarkers of brain tissue injury [42, 43].

Calbindin-1 (CALB1) upregulation indicates severe disruption of calcium homeostasis, as this calcium-buffering protein is typically sequestered intracellularly to regulate calcium levels and prevent excitotoxicity [74]. Its presence in circulation suggests widespread cellular membrane disruption and calcium dysregulation that can propagate neuronal death through excitotoxic mechanisms.

The multifaceted sTBI responses cluster suggests additional cellular damage through nitric oxide synthase 1 (NOS1) upregulation, indicating disrupted NO homeostasis that affects both vascular function and neurotransmission [75]. TNNI3 elevation reflects cardiac involvement secondary to massive catecholamine release, a well-established consequence of severe brain injury that can lead to neurogenic cardiomyopathy [22, 76]. This heightened adrenergic state contributes to adverse outcomes through vasoconstriction, increased intracranial pressure, and systemic cardiovascular instability [77]. Myoglobin (MB) upregulation likely represents a protective response to tissue hypoxia and ischemia, as this oxygen-binding protein facilitates cellular oxygen delivery under compromised conditions [78]. However, excessive myoglobin release can also indicate muscle damage and poses risks for renal complications, highlighting the complex balance between protective and pathological responses in sTBI.

The amidation cluster reflects disrupted neuropeptide processing, a critical post-translational modification required for full biological activity of various hormones and neuropeptides [79]. The presence of CALCA (calcitonin-related polypeptide alpha), ADM (adrenomedullin), and CRH (corticotropin-releasing hormone) demonstrates activation of diverse neuroendocrine stress responses [62, 80, 81]. These peptides regulate vascular tone, stress hormone release, and neuroprotective signaling, suggesting that amidation pathway activation represents an adaptive mechanism attempting to restore homeostasis through enhanced neuropeptide function. However, dysregulated processing may impair the effectiveness of these protective responses, contributing to prolonged pathophysiological dysfunction following sTBI.

Cellular origin of differentially expressed proteins

An important consideration in plasma proteomic studies is determining the cellular origin of DEPs, improving mechanistic understanding of brain-specific and systemic responses. While this study does not directly characterize cellular source, inferences may be made through current literature. We identified intracellular glial-specific markers (e.g. GFAP; astrocytes, S100B; astrocytes and oligodendrocytes) [82, 83] and several inflammatory markers expressed across both peripheral immune cells and activated glial cells, indicating interplay between CNS responses and inflammation (e.g. interleukins, TNF family, C-C motif chemokine ligands) [84, 85]. Several identified markers originate from neurons, indicating cellular damage/dysfunction (e.g. NEFL, NOS, CALCA) [81, 86, 87], and impaired synaptic function/neural development (e.g. VWC2, CALB1, CRH) [56, 88, 89]. Endothelial dysfunction in the blood-brain barrier is suggested through coagulation factors and proteins involved in ECM maintenance, such as VWA1, VWF, ADM [80, 90, 91]. Cell-specific proteomic studies are necessary to confirm cellular localization and elucidate injury mechanisms.

Study limitations

Our study provides comprehensive evaluation of the sTBI proteome in pediatric patients; however, several limitations must be considered. First, we collected plasma samples on day 1 of PICU admission, limiting our ability to track protein expression and pathway alteration changes over extended periods. Additionally, our data does not account for time differences between injury and admission to PICU. However, given the severe nature of these injuries (e.g. motor vehicle crashes), patients were directly admitted from the ER to the PICU, limiting extensive variability between injury date and sample collection time. Second, our limited sample size, which was based on convenience ($n = 20$ per cohort), may have contributed to lack of significance in protein expression between surviving and deceased patients. For example, IL-6 and GFAP have been previously associated with poor patient outcomes [44, 45]. While our machine learning model demonstrated perfect classification between sTBI patients and healthy controls with statistical validation via permutation testing, the sample size also limits its generalizability and independent validation cohorts are required to confirm these findings before clinical deployment. Third, although our study offers valuable insights regarding injury etiology, we did not explicitly match for comorbidities, potentially introducing bias as comorbidities may contribute to altered plasma protein expression. Fourth, our study specifically investigated plasma rather than cerebrospinal fluid, limiting comprehensive analysis of altered sTBI protein expression. Fifth, we did not investigate protein expression in specific cell type contexts, limiting understanding of pathophysiological mechanisms. Finally, our study relies on the Olink platform for protein quantification (PEA), without orthogonal validation. However, we employed methodological rigor through multiple approaches. The Olink protein panel offers highly specific insights into key proteins involved in pathological components of sTBI [92], and PEA provides a highly sensitive, linear antibody-based approach with high specificity based

on the hybridization of two complementary nucleotide tags. We further applied stringent significance cutoffs (FDR-corrected *p*-value, fold change ≥ 4) to ensure robust findings. Furthermore, the Olink platform's pre-selected antibody panel captures only a defined subset of the proteome, which may constrain pathway-level insights and restrict the identification of novel biomarkers compared to unbiased discovery approaches. While traditional mass spectrometry-based proteomics offer more comprehensive proteome coverage, antibody-based methods like PEA identify specific protein targets and provide superior sensitivity for low-abundance proteins [93]. Compared to alternative platforms such as SomaScan, which uses aptamers and has been shown to have lower specificity [94], Olink demonstrates high concordance with direct protein measurements using ELISA and multiplex bead technology [95, 96]. Further comprehensive cell type investigations (e.g., clustering analysis) and metabolomic studies are required for better cellular pathology understanding.

Conclusions

Our study identified various DEPs and pathways that advance understanding of pediatric sTBI pathology. While IL-6 and GFAP are established TBI biomarkers, the current literature lacks mechanistic insights into their roles. We address this gap through pathway enrichment analysis of curated biological databases, revealing specific molecular mechanisms including cytokine-signaling pathways (e.g., interleukins, TNF family), opsonization, and neuronal/astrocytic injury responses. Notably, we identified IL-6 as a central hub connecting inflammatory and neuropathological mechanisms, illustrating its pivotal role in driving injury progression. Furthermore, our pathway-clinical variable correlation analysis bridges the gap between underlying pathophysiological mechanisms and the inherent clinical heterogeneity of sTBI. Finally, we identified several previously under-examined sTBI biomarkers (e.g., VWA1, TNFSF11) that accurately discriminate between sTBI patients and healthy controls.

Supplementary Information The online version contains supplementary material available at https://doi.org/10.1007/s00011-026-02209-6.

Author contributions DDF conceived and designed the study. EC and DDF collected human samples and clinical data. EC, DT, MD, MM, GC and DDF analyzed all data and produced figures. EC and DDF wrote the manuscript with input from all other authors.

Funding DDF received study funding from the GSK Chair in Clinical Pharmacology, the AMOSO Innovation Fund, and a Donor Legacy Gift via the Children's Health Foundation (https://childhealth.ca/).

Data availability The raw proteomic datasets and complete analysis code generated and analyzed for this study are available from the corresponding author upon reasonable request.

Declarations

Conflict of interest The authors declare no competing interests.

Ethical approval This study was approved by the Western University, Human Research Ethics Board (HREB; #17908E; #15996E). Consent was obtained from the legal guardians of all pediatric patients admitted with sTBI, and both guardian consent and patient assent were secured for healthy control participants.

Consent for publication Not applicable.

References

1. Theodorou CM, Galganski LA, Jurkovich GJ, Farmer DL, Hirose S, Stephenson JT, Trappey AF. Causes of early mortality in pediatric trauma patients. J Trauma Acute Care Surg. 2021;90(3):574–81.
2. Neumane S, Camara-Costa H, Francillette L, Araujo M, Toure H, Brugel D, et al. Functional outcome after severe childhood traumatic brain injury: Results of the TGE prospective longitudinal study. Ann Phys Rehabil Med. 2021;64(1):101375.
3. Horn TC, Lundine JP, Busch TA, Benkart RA, Taylor HG, Koterba CH. Long-Term Outcomes of Pediatric Traumatic Brain Injury Following Inpatient Rehabilitation. J Head Trauma Rehabil. 2024;39(2):E95–104.
4. Najem D, Rennie K, Ribecco-Lutkiewicz M, Ly D, Haukenfrers J, Liu Q, et al. Traumatic brain injury: classification, models, and markers. Biochem Cell Biol. 2018;96(4):391–406.
5. McKee AC, Daneshvar DH. The neuropathology of traumatic brain injury. Handb Clin Neurol. 2015;127:45–66.
6. Fedoruk RP, Lee CH, Banoei MM, Winston BW. Metabolomics in severe traumatic brain injury: a scoping review. BMC Neurosci. 2023;24(1):54.
7. Araki T, Yokota H, Morita A. Pediatric Traumatic Brain Injury: Characteristic Features, Diagnosis, and Management. Neurol Med Chir (Tokyo). 2017;57(2):82–93.
8. Goldsmith W, Plunkett J. A biomechanical analysis of the causes of traumatic brain injury in infants and children. Am J Forensic Med Pathol. 2004;25(2):89–100.
9. Morrison G, Fraser DD, Cepinskas G. Mechanisms and consequences of acquired brain injury during development. Pathophysiology. 2013;20(1):49–57.

10. Daley M, Cameron S, Ganesan SL, Patel MA, Stewart TC, Miller MR, et al. Pediatric severe traumatic brain injury mortality prediction determined with machine learning-based modeling. Injury. 2022;53(3):992–8.
11. McBride WR, Conlan CE, Barylski NA, Warneryd AC, Swanson RL. Blood biomarkers in brain injury medicine. Curr Phys Med Rehabil Rep. 2022;10(2):1141–21.
12. Fraser DD, Chen M, Ren A, Miller MR, Martin C, Daley M, et al. Novel severe traumatic brain injury blood outcome biomarkers identified with proximity extension assay. Clin Chem Lab Med. 2021;59(10):1662–9.
13. Zou H, Bao WX, Luo BY. Applications of Proteomics in Traumatic Brain Injury: Current Status and Potential Prospects. Chin Med J (Engl). 2018;131(18):2143–5.
14. Guingab-Cagmat JD, Cagmat EB, Hayes RL, Anagli J. Integration of proteomics, bioinformatics, and systems biology in traumatic brain injury biomarker discovery. Front Neurol. 2013;4:61.
15. Vos PE, Lamers KJ, Hendriks JC, van Haaren M, Beems T, Zimmerman C, et al. Glial and neuronal proteins in serum predict outcome after severe traumatic brain injury. Neurology. 2004;62(8):1303–10.
16. Johnson NH, Hadad R, Taylor RR, Rodriguez Pilar J, Salazar O, Llompart-Pou JA, et al. Inflammatory biomarkers of traumatic brain injury. Pharmaceuticals (Basel). 2022;15(6):660.
17. Ghaith HS, Nawar AA, Gabra MD, Abdelrahman ME, Nafady MH, Bahbah EI, et al. A Literature Review of Traumatic Brain Injury Biomarkers. Mol Neurobiol. 2022;59(7):4141–58.
18. Pignataro G, Sacco Fernandez M, Candelli M, Rozzi G, Piccioni A, Forte E, Franceschi F. Blood-based biomarkers for traumatic brain injury: a new era in diagnosis and prognosis. Int J Mol Sci. 2025;26(24):12158.
19. Daoud H, Alharfi I, Alhelali I, Charyk Stewart T, Qasem H, Fraser DD. Brain injury biomarkers as outcome predictors in pediatric severe traumatic brain injury. Neurocrit Care. 2014;20(3):427–35.
20. Pryzmont M, Kosciuczuk U, Maciejczyk M. Biomarkers of traumatic brain injury: narrative review and future prospects in neurointensive care. Front Med (Lausanne). 2025;12:1539159.
21. Fraser DD, Close TE, Rose KL, Ward R, Mehl M, Farrell C, et al. Severe traumatic brain injury in children elevates glial fibrillary acidic protein in cerebrospinal fluid and serum. Pediatr Crit Care Med. 2011;12(3):319–24.
22. Chen M, Ren AH, Prassas I, Soosaipillai A, Lim B, Fraser DD, Diamandis EP. Plasma Protein Profiling by Proximity Extension Assay Technology Reveals Novel Biomarkers of Traumatic Brain Injury-A Pilot Study. J Appl Lab Med. 2021;6(5):1165–78.
23. Miller MR, Robinson M, Fischer L, DiBattista A, Patel MA, Daley M, et al. Putative Concussion Biomarkers Identified in Adolescent Male Athletes Using Targeted Plasma Proteomics. Front Neurol. 2021;12:787480.
24. Patel MA, Fraser DD, Daley M, Cepinskas G, Veraldi N, Grazioli S. The plasma proteome differentiates the multisystem inflammatory syndrome in children (MIS-C) from children with SARS-CoV-2 negative sepsis. Mol Med. 2024;30(1):51.
25. Spagnolo P, Cela E, Patel MA, Tweddell D, Daley M, Clarson C, et al. Differential expression of plasma proteins and pathway enrichments in pediatric diabetic ketoacidosis. Mol Med. 2025;31(1):4.
26. Stewart TC, Alharfi IM, Fraser DD. The role of serious concomitant injuries in the treatment and outcome of pediatric severe traumatic brain injury. J Trauma Acute Care Surg. 2013;75(5):836–42.
27. Alharfi IM, Charyk Stewart T, Al Helali I, Daoud H, Fraser DD. Infection rates, fevers, and associated factors in pediatric severe traumatic brain injury. J Neurotrauma. 2014;31(5):452–8.
28. Alharfi IM, Stewart TC, Kelly SH, Morrison GC, Fraser DD. Hypernatremia is associated with increased risk of mortality in pediatric severe traumatic brain injury. J Neurotrauma. 2013;30(5):361–6.
29. Alofisan TO, Algarni YA, Alharfi IM, Miller MR, Charyk Stewart T, Fraser DD, Tijssen JA. Paroxysmal Sympathetic Hyperactivity After Severe Traumatic Brain Injury in Children: Prevalence, Risk Factors, and Outcome. Pediatr Crit Care Med. 2019;20(3):252–8.
30. Hochstadter E, Stewart TC, Alharfi IM, Ranger A, Fraser DD. Subarachnoid hemorrhage prevalence and its association with short-term outcome in pediatric severe traumatic brain injury. Neurocrit Care. 2014;21(3):505–13.
31. Brisson AR, Matsui D, Rieder MJ, Fraser DD. Translational research in pediatrics: tissue sampling and biobanking. Pediatrics. 2012;129(1):153–62.
32. Gillio-Meina C, Cepinskas G, Cecchini EL, Fraser DD. Translational research in pediatrics II: blood collection, processing, shipping, and storage. Pediatrics. 2013;131(4):754–66.
33. Lundberg M, Eriksson A, Tran B, Assarsson E, Fredriksson S. Homogeneous antibody-based proximity extension assays provide sensitive and specific detection of low-abundant proteins in human blood. Nucleic Acids Res. 2011;39(15):e102.
34. Assarsson E, Lundberg M, Holmquist G, Bjorkesten J, Thorsen SB, Ekman D, et al. Homogenous 96-plex PEA immunoassay exhibiting high sensitivity, specificity, and excellent scalability. PLoS ONE. 2014;9(4):e95192.
35. Kursa M, Rudnicki W. Feature Selection with the Boruta Package. J Stat Softw. 2010;3611:1–13.
36. Cooke RS, McNicholl BP, Byrnes DP. Use of the Injury Severity Score in head injury. Injury. 1995;26(6):399–400.
37. Arioz BI, Cotuk A, Yaka EC, Genc S. Proximity extension assay-based proteomics studies in neurodegenerative disorders and multiple sclerosis. Eur J Neurosci. 2024;59(6):1348–58.
38. Trautz F, Franke H, Bohnert S, Hammer N, Muller W, Stassart R, et al. Survival-time dependent increase in neuronal IL-6 and astroglial GFAP expression in fatally injured human brain tissue. Sci Rep. 2019;9(1):11771.
39. Yarman S, Soyluk O, Altunoglu E, Tanakol R. Interleukin-6-producing pheochromocytoma presenting with fever of unknown origin. Clin (Sao Paulo). 2011;66(10):1843–5.
40. Akhabir L, Sandford A. Genetics of interleukin 1 receptor-like 1 in immune and inflammatory diseases. Curr Genomics. 2010;11(8):591–606.
41. Glasnovic A, O'Mara N, Kovacic N, Grcevic D, Gajovic S. RANK/RANKL/OPG Signaling in the Brain: A Systematic Review of the Literature. Front Neurol. 2020;11:590480.
42. Yang Z, Wang KK. Glial fibrillary acidic protein: from intermediate filament assembly and gliosis to neurobiomarker. Trends Neurosci. 2015;38(6):364–74.
43. Gafson AR, Barthelemy NR, Bomont P, Carare RO, Durham HD, Julien JP, et al. Neurofilaments: neurobiological foundations for biomarker applications. Brain. 2020;143(7):1975–98.
44. Vos PE, Jacobs B, Andriessen TM, Lamers KJ, Borm GF, Beems T, et al. GFAP and S100B are biomarkers of traumatic brain injury: an observational cohort study. Neurology. 2010;75(20):1786–93.
45. Kumar RG, Diamond ML, Boles JA, Berger RP, Tisherman SA, Kochanek PM, Wagner AK. Acute CSF interleukin-6 trajectories after TBI: associations with neuroinflammation, polytrauma, and outcome. Brain Behav Immun. 2015;45:253–62.
46. Xiong Y, Mahmood A, Chopp M. Current understanding of neuroinflammation after traumatic brain injury and cell-based therapeutic opportunities. Chin J Traumatol. 2018;21(3):137–51.
47. Keegan AD, Leonard WJ, Zhu J. Recent advances in understanding the role of IL-4 signaling. Fac Rev. 2021;10:71.
48. Bhattacharjee A, Shukla M, Yakubenko VP, Mulya A, Kundu S, Cathcart MK. IL-4 and IL-13 employ discrete signaling pathways for target gene expression in alternatively activated monocytes/macrophages. Free Radic Biol Med. 2013;54:1–16.

49. Iyer SS, Cheng G. Role of interleukin 10 transcriptional regulation in inflammation and autoimmune disease. Crit Rev Immunol. 2012;32(1):23–63.
50. Tsitsipanis C, Miliaraki M, Paflioti E, Lazarioti S, Moustakis N, Ntotsikas K, et al. Inflammation biomarkers IL–6 and IL–10 may improve the diagnostic and prognostic accuracy of currently authorized traumatic brain injury tools. Exp Ther Med. 2023;26(2):364.
51. Kinoshita K. Traumatic brain injury: pathophysiology for neurocritical care. J Intensive Care. 2016;4:29.
52. Zehtabchi S, Soghoian S, Liu Y, Carmody K, Shah L, Whittaker B, Sinert R. The association of coagulopathy and traumatic brain injury in patients with isolated head injury. Resuscitation. 2008;76(1):52–6.
53. D'Souza UM, Strange PG. pH dependence of ligand binding to D2 dopamine receptors. Biochemistry. 1995;34(41):13635–41.
54. Goodman GW, Devlin P, West BE, Ritzel RM. The emerging importance of skull-brain interactions in traumatic brain injury. Front Immunol. 2024;15:1353513.
55. Arribat Y. Genetic alterations of VWA1: a new link between extracellular matrix and neuromuscular diseases. Brain. 2021;144(2):362–5.
56. Koike N, Kassai Y, Kouta Y, Miwa H, Konishi M, Itoh N. Brorin, a novel secreted bone morphogenetic protein antagonist, promotes neurogenesis in mouse neural precursor cells. J Biol Chem. 2007;282(21):15843–50.
57. Lee WH, Seo D, Lim SG, Suk K. Reverse Signaling of Tumor Necrosis Factor Superfamily Proteins in Macrophages and Microglia: Superfamily Portrait in the Neuroimmune Interface. Front Immunol. 2019;10:262.
58. Zhang J, Jiang R, Liu L, Watkins T, Zhang F, Dong JF. Traumatic brain injury-associated coagulopathy. J Neurotrauma. 2012;29(17):2597–605.
59. Zhang D, Gong S, Jin H, Wang J, Sheng P, Zou W, et al. Coagulation Parameters and Risk of Progressive Hemorrhagic Injury after Traumatic Brain Injury: A Systematic Review and Meta-Analysis. Biomed Res Int. 2015;2015:261825.
60. Kriz J, Zhu Q, Julien JP, Padjen AL. Electrophysiological properties of axons in mice lacking neurofilament subunit genes: disparity between conduction velocity and axon diameter in absence of NF-H. Brain Res. 2000;885(1):32–44.
61. Ozkaynak E, Abello G, Jaegle M, van Berge L, Hamer D, Kegel L, et al. Adam22 is a major neuronal receptor for Lgi4-mediated Schwann cell signaling. J Neurosci. 2010;30(10):3857–64.
62. Aguilera G, Liu Y. The molecular physiology of CRH neurons. Front Neuroendocrinol. 2012;33(1):67–84.
63. Thau L, Asuka E, Mahajan K. Physiology. Opsonization. StatPearls. Treasure Island (FL)2025.
64. Wright SD, Ramos RA, Patel M, Miller DS. Septin: a factor in plasma that opsonizes lipopolysaccharide-bearing particles for recognition by CD14 on phagocytes. J Exp Med. 1992;176(3):719–27.
65. Gershov D, Kim S, Brot N, Elkon KB. C-Reactive protein binds to apoptotic cells, protects the cells from assembly of the terminal complement components, and sustains an antiinflammatory innate immune response: implications for systemic autoimmunity. J Exp Med. 2000;192(9):1353–64.
66. Diniz SN, Nomizo R, Cisalpino PS, Teixeira MM, Brown GD, Mantovani A, et al. PTX3 function as an opsonin for the dectin-1-dependent internalization of zymosan by macrophages. J Leukoc Biol. 2004;75(4):649–56.
67. Tanaka M, Miyajima A, Oncostatin M. a multifunctional cytokine. Rev Physiol Biochem Pharmacol. 2003;149:39–52.
68. Molnarfi N, Benkhoucha M, Funakoshi H, Nakamura T, Lalive PH. Hepatocyte growth factor: A regulator of inflammation and autoimmunity. Autoimmun Rev. 2015;14(4):293–303.
69. Arruda-Silva F, Bianchetto-Aguilera F, Gasperini S, Polletti S, Cosentino E, Tamassia N, Cassatella MA. Human Neutrophils Produce CCL23 in Response to Various TLR-Agonists and TNFalpha. Front Cell Infect Microbiol. 2017;7:176.
70. Panopoulos AD, Watowich SS. Granulocyte colony-stimulating factor: molecular mechanisms of action during steady state and 'emergency' hematopoiesis. Cytokine. 2008;42(3):277–88.
71. Petri B, Broermann A, Li H, Khandoga AG, Zarbock A, Krombach F, et al. von Willebrand factor promotes leukocyte extravasation. Blood. 2010;116(22):4712–9.
72. Schoeps B, Eckfeld C, Prokopchuk O, Bottcher J, Haussler D, Steiger K, et al. TIMP1 Triggers Neutrophil Extracellular Trap Formation in Pancreatic Cancer. Cancer Res. 2021;81(13):3568–79.
73. Liu H, Sun L, Zhao H, Zhao Z, Zhang S, Jiang S, et al. Proteinase 3 depletion attenuates leukemia by promoting myeloid differentiation. Cell Death Differ. 2024;31(6):697–710.
74. Rai V, Mendoza-Mari Y, Brazdzionis J, Radwan MM, Connett DA, Miulli DE, Agrawal DK. Transcriptomic Analysis of Gene Expression and Effect of Electromagnetic Field in Brain Tissue after Traumatic Brain Injury. J Biotechnol Biomed. 2024;7(1):101–10.
75. Kozlov AV, Bahrami S, Redl H, Szabo C. Alterations in nitric oxide homeostasis during traumatic brain injury. Biochim Biophys Acta Mol Basis Dis. 2017;1863(10 Pt B):2627–32.
76. Rimaz S, Ashraf A, Marzban S, Haghighi M, Zia Ziabari SM, Biazar G, et al. Significance of Cardiac Troponin I Elevation in Traumatic Brain Injury Patients. Anesth Pain Med. 2019;9(2):e90858.
77. Singh A, Prajapati HP, Kumar R, Singh NP, Kumar A. Prognostic Role of Catecholamine in Moderate-to-Severe Traumatic Brain Injury: A Prospective Observational Cohort Study. Asian J Neurosurg. 2022;17(3):435–41.
78. Xie LK, Yang SH. Brain globins in physiology and pathology. Med Gas Res. 2016;6(3):154–63.
79. Chufan EE, De M, Eipper BA, Mains RE, Amzel LM. Amidation of bioactive peptides: the structure of the lyase domain of the amidating enzyme. Structure. 2009;17(7):965–73.
80. Ihara M, Washida K, Yoshimoto T, Saito S, Adrenomedullin. A vasoactive agent for sporadic and hereditary vascular cognitive impairment. Cereb Circ Cogn Behav. 2021;2:100007.
81. Mehkri Y, Hanna C, Sriram S, Lucke-Wold B, Johnson RD, Busl K. Calcitonin gene-related peptide and neurologic injury: An emerging target for headache management. Clin Neurol Neurosurg. 2022;220:107355.
82. Sacco MA, Gualtieri S, Tarallo AP, Verrina MC, Calafiore J, Princi A, et al. The role of GFAP in post-mortem analysis of traumatic brain injury: a systematic review. Int J Mol Sci. 2024;26(1):185.
83. Steiner J, Bernstein HG, Bielau H, Berndt A, Brisch R, Mawrin C, et al. Evidence for a wide extra-astrocytic distribution of S100B in human brain. BMC Neurosci. 2007;8:2.
84. Burkhart A, Helgudottir SS, Mahamed YA, Fruergaard MB, Holm-Jacobsen JN, Haraldsdottir H, et al. Activation of glial cells induces proinflammatory properties in brain capillary endothelial cells in vitro. Sci Rep. 2024;14(1):26580.
85. Sanmarco LM, Polonio CM, Wheeler MA, Quintana FJ. Functional immune cell-astrocyte interactions. J Exp Med. 2021;218(9):e20202715.
86. Wong KR, O'Brien WT, Sun M, Yamakawa G, O'Brien TJ, Mychasiuk R, et al. Serum Neurofilament Light as a Biomarker of Traumatic Brain Injury in the Presence of Concomitant Peripheral Injury. Biomark Insights. 2021;16:11772719211053449.
87. Tricoire L, Vitalis T. Neuronal nitric oxide synthase expressing neurons: a journey from birth to neuronal circuits. Front Neural Circuits. 2012;6:82.
88. Acharya M, Singh N, Gupta G, Tambuwala MM, Aljabali AAA, Chellappan DK, et al. Vitamin D, Calbindin, and calcium

signaling: Unraveling the Alzheimer's connection. Cell Signal. 2024;116:111043.
89. Nezi M, Mastorakos G, Mouslech Z et al. Corticotropin Releasing Hormone And The Immune/Inflammatory Response. In: Feingold KR, Adler RA, Ahmed SF, Anawalt B, Blackman MR, Chrousos G, editors. Endotext. South Dartmouth (MA)2000.
90. Fitzgerald JWARP. A Unique Extracellular Matrix Component of Cartilage, Muscle, and Endothelial Cell Basement Membranes. Anat Rec (Hoboken). 2020;303(6):1619–23.
91. Xu X, Kozar R, Zhang J, Dong JF. Diverse activities of von Willebrand factor in traumatic brain injury and associated coagulopathy. J Thromb Haemost. 2020;18(12):3154–62.
92. Wik L, Nordberg N, Broberg J, Bjorkesten J, Assarsson E, Henriksson S, et al. Proximity Extension Assay in Combination with Next-Generation Sequencing for High-throughput Proteome-wide Analysis. Mol Cell Proteom. 2021;20:100168.
93. Wang H, Zhao T, Zeng J, Zhang R, Pu L, Qian S, et al. Methods and clinical biomarker discovery for targeted proteomics using Olink technology. Proteom Clin Appl. 2024;18(5):e2300233.
94. Katz DH, Robbins JM, Deng S, Tahir UA, Bick AG, Pampana A, et al. Proteomic profiling platforms head to head: Leveraging genetics and clinical traits to compare aptamer- and antibody-based methods. Sci Adv. 2022;8(33):eabm5164.
95. Olink. Measuring protein biomarkers with Olink — technical comparisons and orthogonal validation. 2021.
96. Olink. Multiplex analysis of inflammatory proteins: A comparative study across multiple platforms. 2022.

Authors and Affiliations

Enis Cela[1] · David Tweddell[2] · Mark Daley[2,3] · Maria Morello[4] · Gediminas Cepinskas[5,6,7] · Douglas D. Fraser[1,7,8,9,10,11,12]

✉ Douglas D. Fraser
douglas.fraser@lhsc.on.ca

[1] Physiology & Pharmacology, Western University, London, ON N6A 3K7, Canada

[2] Computer Science, Western University, London, ON N6A 3K7, Canada

[3] Epidemiology and Biostatistics, Western University, London, ON N6A 3K7, Canada

[4] Experimental Medicine, University of Rome Tor Vergata, 00133 Rome, Italy

[5] Medical Biophysics, Western University, London, ON N6A 3K7, Canada

[6] Anatomy and Cell Biology, Western University, London, ON N6A 3K7, Canada

[7] London Health Sciences Centre Research Institute, London, ON N6C 2R5, Canada

[8] Pediatrics, Western University, London, ON N6A 3K7, Canada

[9] Children's Health Research Institute, London, ON N6C 4V3, Canada

[10] Clinical Neurological Sciences, Western University, London, ON N6A 3K7, Canada

[11] GSK Chair in Clinical Pharmacology, Western University, London, ON N6A 3K7, Canada

[12] Room A5-132, Victoria Research Laboratories, 800 Commissionaires Road East, London, ON N6A 5W9, Canada